ISSN 1023-1935, Russian Journal of Electrochemistry, 2019, Vol. 55, No. 1, pp. 34–43. © Pleiades Publishing, Ltd., 2019.
Published in Russian in Elektrokhimiya, 2019, Vol. 55, No. 1, pp. 39–50.

Further Thoughts on Turbulent Flow in a Pipe[1]

John Newman*

Department of Chemical and Biomolecular Engineering, University of California, Berkeley, California, 94720-1462 USA

**e-mail: newman@newman.cchem.berkeley.edu*

Received February 9, 2018; revised April 18, 2018; accepted May 8, 2018

Abstract—Nikuradse's 1932 paper on turbulent flow in a smooth pipe contains a wealth of information on flow resistance (friction factor) and profiles of velocity and eddy viscosity. The goal here is to study this information in detail with the objective of applying it to other turbulent-flow situations. In particular, reverse engineering supports a value of $n = 2$ for the exponent on the volumetric dissipation in the decay term of the equation of the dissipation theorem. Of equal importance, integration of Nikuradse's profiles of eddy viscosity does not lead to his formula for the universal resistance law; instead the presence of the viscous sublayer has an overt effect on the result even though we had thought that such a region influenced only the form of mass transfer at high values of the Schmidt number. A formula is proposed for the decay of dissipation for turbulent flow in smooth pipes.

Keywords: fluid mechanics, turbulence, dissipation, mass transfer

DOI: 10.1134/S1023193519010105

INTRODUCTION

The dissipation theorem refers to the statistical representation of turbulence by the Reynolds stress, the volumetric dissipation $\tau : \nabla \mathbf{v}$, the eddy viscosity, and the kinetic energy per unit volume. [1] introduces the dissipation theorem and applies it to data on mass transfer in the rotating-cylinder system. [2] applies these concepts to turbulent flow in a pipe. One basic equation of the dissipation theorem relates the volumetric dissipation to the eddy viscosity. For pipe flow, this takes the dimensionless form

$$D = \frac{\xi^2}{1 + R^+ M}, \tag{1}$$

where $D = \mu \mathscr{D}_V / \tau_0^2$, $\mathscr{D}_V$ being the dissipation per unit volume, μ the viscosity, and τ_0 the shear stress at the wall of the tube. R^+ is the independent stress parameter $(R/\nu)(\tau_0/\rho)^{0.5}$, and R^+M is the ratio $\nu^{(t)}/\nu$ of the eddy kinematic viscosity to the kinematic viscosity. $\xi = r/R$ is the radial position divided by the radius of the pipe. The second basic equation describes how the volumetric dissipation varies in time and space due to convection, diffusion, and decay. For steady, fully developed flow in a pipe, the equation becomes

$$\frac{1}{\xi}\frac{\partial}{\partial \xi}\left(\xi^3 \frac{\partial \ln D}{\partial \xi}\right) = \Lambda \frac{D^n}{\xi^p (R^+)^q} = \text{decay}. \tag{2}$$

Equations (1) and (2) are essentially Eqs. (49) and (50) in [2]. The dimensionless decay is defined by the left side of Eq. (2). Λ is a dimensionless rate constant, n is the reaction order for decay, and the two terms in the denominator have been added so as to provide flexibility. There is also a term 4, not shown here, which if included allows laminar flow to be a solution of Eq. (2). $D = 1$ at $\xi = 1$, the wall of the pipe, and D becomes proportional to ξ^2 as $\xi \to 0$.

From turbulent pipe flow, we learned that the exponent used in the divergence should remain 1, as is appropriate for the cylindrical geometry, and not become 5 for the rotating cylinders or –1 for pipe flow. Furthermore, the result for the eddy viscosity should be able to superpose for different values of the stress level (at least for high Reynolds numbers), and this can be accomplished by introducing factors into the decay term with the exponents p and q for the radial position and for the stress level (R^+). We also learn more about how negative values of the eddy viscosity could arise in the calculations and how this could be avoided. The objective is to learn how to apply similar changes to other situations of turbulent flow. However, there is more information to be gleaned from Nikuradse's 1932 paper [3].

The focus here is on pipe flow, dealing with items not adequately discussed in [2]. First, plot all of Nikuradse's distributions of eddy viscosity at different Reynolds numbers, from 4000 to 3.2×10^6. This covers a range of R^+ from 112 to 56000.

[1] The article is published in the original.

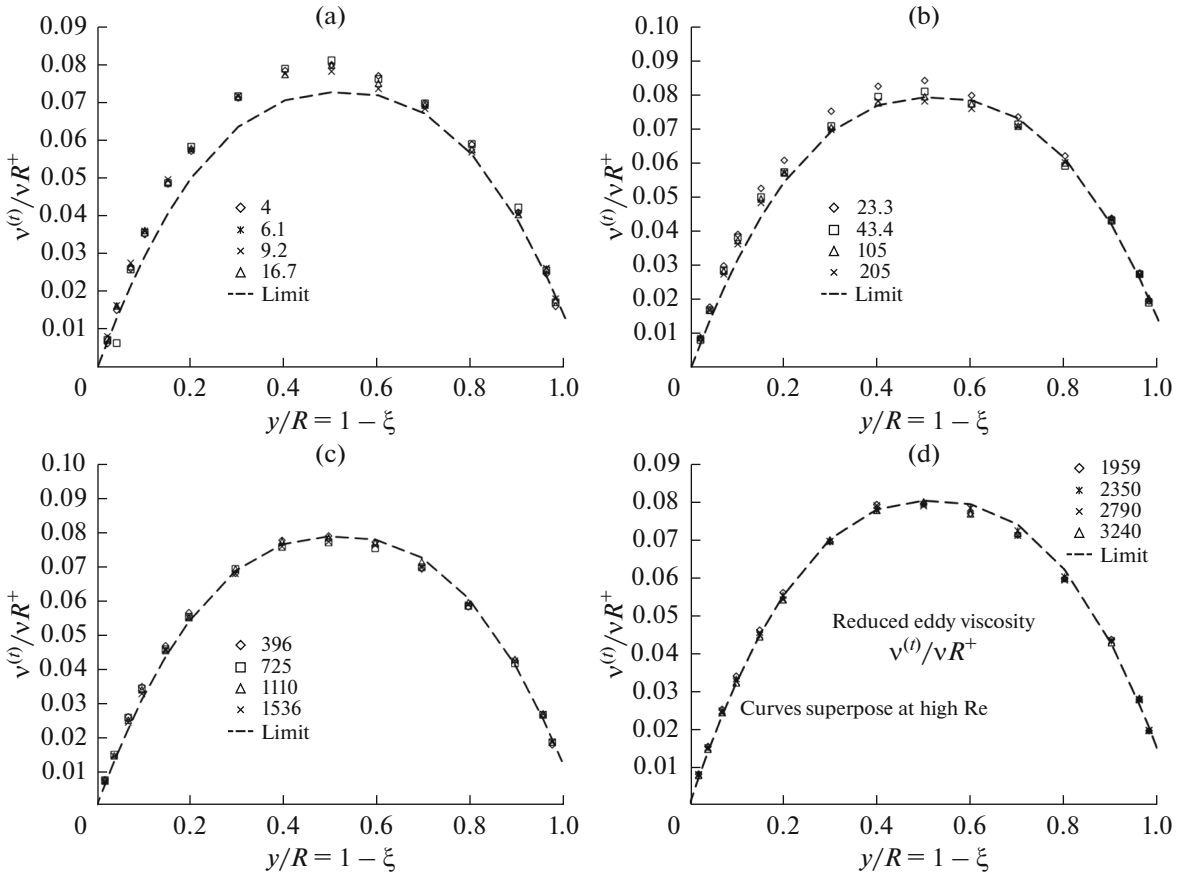

Fig. 1. The eddy-viscosity profiles of Nikuradse for 16 different Reynolds numbers. The dashed line is the limit curve for large Reynolds numbers. Points for the lower Reynolds numbers generally lie slightly higher than the limit curve. (a) is for Reynolds numbers of 4000, 6100, 9200, and 16700. (b) is for Reynolds numbers of 23300, 43400, 105000, and 205000. (c) is for Reynolds numbers of 396000, 725000, 1110000, and 1536000. d is for the high Reynolds numbers of 1959000, 2350000, 2790000, and 3240000.

The curves have much the same shape throughout the entire range of Reynolds numbers. This means that the eddy-viscosity profiles are approximately superposable if one first divides by the stress parameter R^+. The flow is well characterized by these profiles. For example, the friction factor f is given by the formula B5, derived in Appendix B,

$$\sqrt{\frac{2}{f}} = R^+ \int_0^1 \frac{\xi^3 d\xi}{1 + R^+ M(\xi)}, \qquad (3)$$

where $\xi = r/R$ and $M = \nu^{(t)}/\nu R^+$.

From Fig. 1 it is evident that Nikuradse [3] believes that the eddy viscosity does not go to zero at the center line. In light of the author's proof that it should go to zero (see [2]), the data might indicate that the flow is not really fully developed, that is, there are still some entrance-length effects. It should be noted that Fig. 1 covers a wide range of Reynolds numbers and several pipe sizes and that the profiles are more noted by their similarity than by any possible random situation of developing flow. (This might prompt one to try to move on quickly to the later phases of this investigation, of developing flows on a rotating disk or a flat plate at zero incidence or, in the present example, pipe flow.) One should probably keep clearly in mind the message from Nikuradse that the eddy viscosity does not go exactly to zero at the center line. [This observation might have implications for the issue of y^3 or y^4 for the decay of eddy viscosity near a solid wall. The argument supporting y^4 depends on fully developed flow and the invariance of certain statistical averages with axial distance. The strong support for y^3 dependence comes from the observed dependence of the Stanton number on the 2/3rd power of the Schmidt number. See for example [1].

REVERSE ENGINEERING OF NIKURADSE'S RESULTS

Even in Fig. 9 of [2] we obtained a good idea of the profile of the volumetric dissipation by applying Eq. (1) to the limit curve of Nikuradse. The previously unpublished Appendix A is included here because it

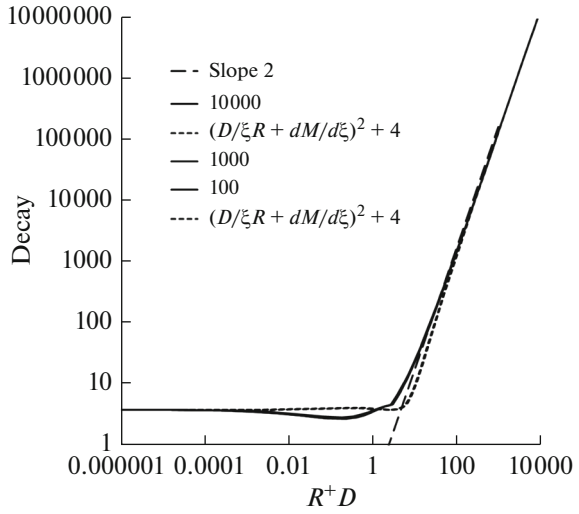

Fig. 2. The dimensionless decay calculated by reverse engineering from the limit curve for eddy viscosity in pipe flow as measured experimentally by Nikuradse, and as fitted by John Newman. The short-dashed curve shows a close approximation. The long-dashed line shows that the slope is 2 for large values of R^+D. Calculated curves overlap for three values of R^+. Two approximations overlap for two values of R^+.

gives a very good idea of the radial distribution of D and shows clearly a number of regions of different behavior of D. Similar reverse engineering can also reveal the form of the decay term. For an approximation to the eddy-viscosity profile of Nikuradse, use the formula

$$M = \nu^{(t)}/\nu R^+ = 0.08 - 0.38431\left|\xi - 0.48\right|^{2.4}. \quad (4)$$

The corresponding fit for a curve which goes to zero on the axis is

$$\nu^{(t)}/\nu R^+ = 0.08 - 0.42224\left|\xi - 0.5\right|^{2.4}. \quad (5)$$

The reverse engineering involves obtaining D by substituting Eq. (4) into Eq. (1) and then substituting the result into Eq. (2) to get the decay. This produces a multitude of values of the decay term at positions and Reynolds numbers encountered in Nikuradse's work, and it gives a hint of what would be a suitable representation of the decay term as a function of the volumetric dissipation. Here are some of the necessary derivatives.

$$\frac{\partial D}{\partial \xi} = \frac{2\xi}{1+MR^+} - \frac{\xi^2}{[1+MR^+]^2}R^+\frac{\partial M}{\partial \xi} = \frac{2D}{\xi} - \frac{D^2}{\xi^2}R^+\frac{\partial M}{\partial \xi}, \quad (6)$$

$$\frac{\partial^2 D}{\partial \xi^2} = \frac{2}{1+MR^+} - \frac{4\xi}{[1+MR^+]^2}R^+\frac{\partial M}{\partial \xi} + \frac{2\xi^2}{[1+MR^+]^3}\left(R^+\frac{\partial M}{\partial \xi}\right)^2 - \frac{\xi^2}{[1+MR^+]^2}R^+\frac{\partial^2 M}{\partial \xi^2} = \frac{2D}{\xi^2} - \frac{4D^2}{\xi^3}R^+\frac{\partial M}{\partial \xi} + \frac{2D^3}{\xi^4}\left(R^+\frac{\partial M}{\partial \xi}\right)^2 - \frac{D^2}{\xi^2}R^+\frac{\partial^2 M}{\partial \xi^2}. \quad (7)$$

Without worry about signs with the absolute value, the derivatives of M are

$$\frac{\partial M}{\partial \xi} = -0.38431\times 2.4\left|\xi - 0.48\right|^{1.4}. \quad (8)$$

$$\frac{\partial^2 M}{\partial \xi^2} = -0.38431\times 2.4\times 1.4\left|\xi - 0.48\right|^{0.4}. \quad (9)$$

The sign of the first derivative changes at $\xi = 0.48$. One should probably refit Nikuradse's limit curve with a series of even powers of ξ, to eliminate this (probably nonphysical) fractional power of 2.4.

Thus, one can write for the (dimensionless) decay

$$\text{decay} = 3\left(\frac{\xi}{D}\frac{\partial D}{\partial \xi}\right) - \left(\frac{\xi}{D}\frac{\partial D}{\partial \xi}\right)^2 + \frac{\xi^2}{D}\frac{\partial^2 D}{\partial \xi^2}. \quad (10)$$

Substitution of Eqs. (8) and (9) gives

$$\text{decay} = 4 - 3\left(\frac{DR^+}{\xi}\frac{\partial M}{\partial \xi}\right) + \left(\frac{DR^+}{\xi}\frac{\partial M}{\partial \xi}\right)^2 - DR^+\frac{\partial^2 M}{\partial \xi^2}. \quad (11)$$

The number 4 appears again here.

This has been implemented in a spreadsheet. Results are shown in Fig. 2.

First, Fig. 2 provides strong evidence that the decay term should be proportional to D^2, particularly for large values of R^+D, which are the values of most interest in the wall region where the volumetric dissipation decreases dramatically. The figure also suggests that the decay term does depend only on R^+D. Second, Fig. 2 supports the idea that a term 4 needs to be included in the decay term for small values of R^+D, although this term may not be significant with high levels of turbulence. This term does not work well in reproducing the shape of Nikuradse's eddy-viscosity curves in Fig. 1, even though it comes from reverse engineering with his limit curve. The approximation shown by the short-dashed curve on Fig. 2 is

$$\text{decay approximation} = 4 + \left(\frac{DR^+}{\xi}\frac{\partial M}{\partial \xi}\right)^2, \quad (12)$$

thus picking two significant terms from Eq. (11). Consequently, a third lesson from Fig. 2 is that the decay term includes an explicit dependence on ξ (which could come from the local stress) and, even more sur-

prisingly, a dependence on the derivative $dM/d\xi$. Normally we do not think of the decay term as being related to such a derivative, implying a nonlocal dependence. (We are bothered by a similar appearance of a derivative of chemical potential in the theory of Cahn and Hilliard [4] on the size distribution of droplets resulting from supercritical condensation.) One can combine the R^+ again with the derivative and say that the decay is shown to depend on the derivative of $\nu^{(t)}$, which translates to a derivative of D by Eqs. (1) or (6). (See Eq. (10).) A second useful approximation to the decay is

$$\text{decay approximation} = 4 + 0.17\left(\frac{DR^+}{\xi}\right)^2, \qquad (13)$$

which matches exactly with what we had arrived at by exhaustive comparison of various forms with Nikuradse's experimental determination of the friction factor for pipe flow. Here the derivative of M has been eliminated, and the value of Coef is taken to be 0.17. Thus we conclude that $n = 2$, at least for pipe flow.

However, Eq. (13) leads to negative values for the eddy viscosity near the center line and for small values of R^+, and generally to a zero value for the eddy viscosity on the axis, as in Eq. (5). This forces us to the conclusion that Nikuradse is probably right, that the eddy viscosity does not go exactly to zero on the center line.

This thought prompted new ideas of how to influence the shape. One is to have an exponent n of 2 (which can give the straight lines on the universal-resistance plot) but also an exponent of 1, which might be closer to decay of homogeneous isotropic turbulence in the final stages of decay. This can be expressed in an equation of the form

$$\text{decay approximation} = C_2\left(R^+D/\xi\right)^2 + C_1\,R^+D/\xi, \qquad (14)$$

where Coef has been replaced by C_2 and a new term with C_1 has been added. The term 4 may or may not be helpful. It is apparent that Eq. (14) strongly resembles Eq. (11), already obtained by reverse engineering of Eq. (4). (Perhaps a term like C_0R^+D is also needed.)

The miracle from Nikuradse's work is that the derivative of M at the pipe wall is insensitive to the value of R^+. This is in harmony with earlier work in the 1920s on the universal velocity profile. It is a necessary condition for the validity of the universal resistance law, which is treated here in Appendix B. It may not apply to other turbulent flows.

For pipe flow, $\overline{\tau}_{rz} = \tau_0 r/R = \xi\tau_0$. Hence, we can associate the appearance of ξ in the expressions for the decay with a local stress term in the denominator.

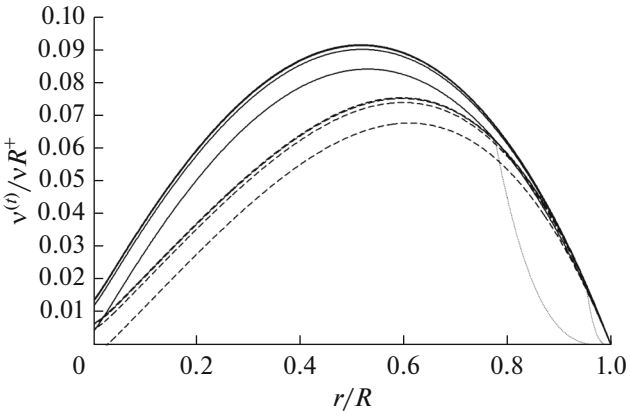

Fig. 3. Profiles of the eddy viscosity calculated with the dissipation theorem. The upper solid curves are calculated with the parameters Coef = 0.17, $n = p = q = 2$, $B^+ = 0.0005$, and $\varepsilon = 0.33/R^+$. Curves for R^+ of 88198, 16399, 3049, and 567 superpose, while that for 105 falls a little lower. (In contrast, Nikuradse's experimental data for low R^+ in Fig. 1 fall above his limit curve.) The solid curves are calculated by the dissipation theorem without regard for any viscous sublayer. Dotted curves for $R^+ = 567$ and 105 show the effect of splicing in the viscous sublayer. For $R^+ = 105$, this extends out from $r/R = 1$ to about 0.8, but much less far for $R^+ = 567$. At the left, the curves mimic the curves of Nikuradse in Fig. 1 by not going to zero on the axis. This is accomplished by the ε parameter, introduced here. The dashed curves result when the term 4 is added into the dimensionless decay term in the dissipation equation.

Thus, we can express the approximate decay term by the equation

$$\text{dimensional decay} = \frac{\tau_0^2}{\rho R^2}\text{decay} \approx \frac{k\tau_0}{\rho}\left(\frac{\mu D_V}{R\overline{\tau}_{rz}}\right)^2. \qquad (15)$$

The local stress has a different radial dependence for rotating cylinders ($\overline{\tau}_{r\theta} = \tau_i/\xi^2$), and this association of ξ with local stress may be helpful. The principal difference between pipe flow and rotating cylinders is in this radial dependence of the local stress.

RESULTS WITH THE DISSIPATION THEOREM

Graphs of the prediction of the distribution of eddy viscosity from the dissipation theorem are shown in Fig. 3. (Equation (14) is implemented in a form equivalent to replacing D^n with $D^n + \varepsilon D$ in the decay term, where $\varepsilon = C_3/R^+$. This is not quite the same, and we need to see exactly how we want Eq. (14) to be written.) These graphs show a nice shape (for $n = 2$) but are not quite as fat as the profiles shown in Fig. 1, from Nikuradse. They do reproduce the nonzero value of the eddy viscosity on the center line. For $n = 2$, the profiles give a friction-factor plot with a straight line

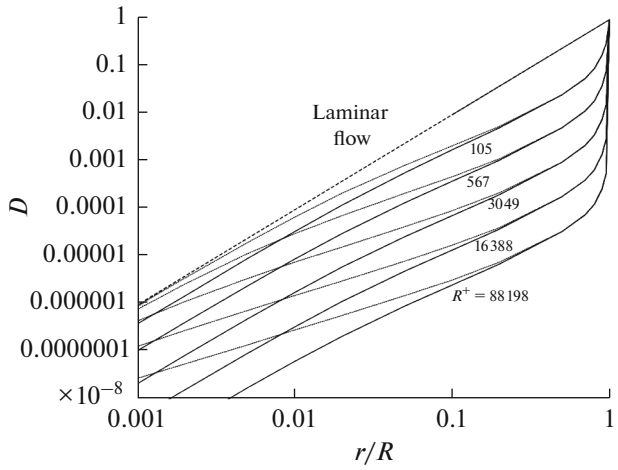

Fig. 4. The solid curves represent the volumetric dissipation calculated by Eq. (1) from Nikuradse's limit curve for the eddy viscosity, as represented by Eq. (4). The short dashed curves are calculated the same way but from Eq. (5), where the eddy viscosity is forced to be zero on the axis. The line with long dashes is the curve for laminar flow and necessarily has a zero value for the eddy viscosity. Hence, crossing the laminar line creates negative values for the eddy viscosity. All the curves start at 1 at the wall ($r/R = 1$). Higher values of R^+ cause a steeper drop in the volumetric dissipation and thereby stay farther away from the region of negative eddy viscosity. However, the curves with zero eddy viscosity on the center line approach asymptotically the laminar line near the axis. This means that the dissipation program, which predicts the eddy viscosity, has a greater likelihood of touching the laminar line.

for large Reynolds number when plotted in the manner of the law of universal resistance. Other values of n make it hard to achieve such a straight line. In attempts to modify the shape of the distribution of eddy viscosity, the term which permits the laminar flow to be a solution of the dissipation differential equation was added. As discussed further below, this modification of the eddy-viscosity profile does not greatly affect the shape of the friction factor versus Re or R^+. (What we are getting now with the added 4 term is shown by dashed lines on Fig. 3.)

AVOIDING NEGATIVE EDDY VISCOSITY

In the preparation of Fig. 3, negative values of the eddy viscosity were encountered, close to the axis and at low values of R^+, when running the dissipation-theorem calculations. This was with a decay term that looks like Eq. (13) (with or without the added 4). There should be a physical mechanism that prevents negative values from occurring. In this regard, Nikuradse's profiles in Fig. 1 with a nonzero eddy viscosity on the axis look more promising. This can be seen in Fig. 4 where Eq. (1) is used to calculate the dissipation from Nikuradse's limit curve (Eq. (4)) and from this curve when the eddy viscosity is forced to zero on the axis (Eq. (5)).

Originally we had expected the eddy viscosity to be a maximum on the center line, but Nikuradse's experimental results (Fig. 1) show that the eddy viscosity actually goes through a maximum and approaches a small but nonzero value on the axis. The decay increases when the dissipation is large near the wall, and it increases even faster closer to the axis (due to the ξ^2 in the denominator). The shape of the dissipation curves in Fig. 4 reflects the decrease of D toward the axis but also the increase in the decay due to the radial position. When D becomes very small, the decay becomes small, and the curve can cross the laminar line.

My reasoning was that the decay term should not continue to decrease as D^2 near the axis; the decay term might decrease only linearly with D in the final stages of decay. That was the reason for introducing the term with εD. Implementing this in the construction of Fig. 3 permitted matching with Nikuradse's nonzero value of the eddy viscosity on the axis, and this also led to the avoidance of the negative values of the eddy viscosity near the axis for low values of R^+. The empirical fit suggests that ε should be inversely proportional to R^+. (The parameters were not changed when making the dashed curves with the extra 4 in the decay. Consequently, the eddy viscosity falls below Nikuradse's values on the axis, and for the lowest value of R^+ negative values are found near the axis.)

Further consideration of these questions leads us to reconsider the decay term. Equation (11) shows that there is a dominant term proportional to $(R^+D)^2$ but there are also two terms proportional to R^+D. One can consider that the derivatives of M should really be evaluated near the wall. Then, $dM/d\xi = -\beta_0 \approx -0.36823$, and $d^2M/d\xi^2$ is about -0.994, so that the full expression of Eq. (9) could be taken to be decay $\approx 4 + (\beta_0 R^+D/\xi)^2 + 3\beta_0\, R^+D/\xi + 0.994\, R^+D$. This makes us think of Coef as approximately equal to $\beta_0{}^2$ and correspondingly for the term proportional to R^+D. We shall, however, continue to use empirical constants for these coefficients.

CALCULATION OF THE FRICTION FACTOR FROM A SPECIFIED DISTRIBUTION OF THE EDDY VISCOSITY

Equation (3) permits the friction factor to be calculated directly from the eddy viscosity. Appendix B shows how to use this equation to derive the relationship of the universal resistance formula. Here we look into how to carry out the calculation numerically with due consideration of the fact that the integrand changes dramatically for small values of $1 - \xi$, from 1 at $\xi = 1$ to something much smaller if R^+ is large. When the integrand is plotted against $R^+(1 - \xi)$, curves for different values of R^+ superpose for small values of the abscissa. A strategy is to use a small step size h for the

first step (such as $0.001/R^+$) and then increase it by a factor of 1.05 for each subsequent step. This allows accurate integration for small values of the abscissa but keeps the total number of steps modest for large values of R^+. The resulting plot, expressed as suggested by the universal resistance law, is shown in the lower curves in Fig. 5. (This new spacing of points gave insufficient accuracy near $\xi = 0$, where negative eddy viscosity could result for small values of R^+. This is not a problem where the eddy viscosity is known or specified, but it can be a problem when using the dissipation theorem to predict the eddy viscosity.)

The discrepancy between the two methods of calculating the friction factor is resolved by careful examination of the details of the integration. There is a difference in the eddy-viscosity profiles in the y^3 region very close to the wall. (See [1] for a description.) The lower curve uses Eq. (3) for direct integration of the eddy-viscosity profiles of Nikuradse as given by Eq. (4). There is no provision for a y^3 region, and the curve falls well below the upper dashed line representing how Nikuradse fit his experimental friction-factor data to the universal resistance law. The upper curve is calculated by means of the dissipation theorem (Eqs. (1) and (2)) with one or two adjustable parameters, and automatic inclusion of the y^3 region.

Other curves (omitted from the graph for clarity) can use Nikuradse's eddy-viscosity profiles but with the y^3 region grafted in. This clearly accounts for the difference between the curves on Fig. 5.

The result elucidated in Fig. 5 is remarkable. We had assumed that the y^3 region was so small that it influences mainly mass transfer at high Schmidt numbers, where the inner part of the diffusion layer near the wall can be explored. The conclusion was that it did not influence very much the hydrodynamics, as embodied in the friction factor. We had included the y^3 region in the dissipation program, which is also used to predict mass-transfer results, and the parameter used ($B^+ = 0.0005$) was a remnant of those investigations. The earlier conclusion (that the viscous sublayer does not affect the hydrodynamics and the friction factor) was not valid. Actual integration of the eddy-viscosity profile as inferred from Fig. 1 does not yield the friction factor as implied by the universal-resistance plot (or by a plot of the friction factor versus the Reynolds number). The y^3 region, narrow as it is, still provides a hydrodynamic resistance sufficient to change greatly the intercept in the universal-resistance law (from about −6.46 to +2). Changing B^+ from 0.0005 to 0.0002 or 0.001 greatly changes the upper curve. (Alternatively, one can assume a y^4 region and put the curve on top of the curve with the y^3 region. The resolution is not sufficient with the friction factor to decide which is better, y^3 or y^4.)

We should expand on the statement that the viscous sublayer has a dramatic effect on the friction factor, since this is an important discovery of this paper. In hindsight it may be obvious that this is true since the friction factor (or the wall stress) results by a straightforward integration of the profile of the eddy viscosity. Nevertheless, we generally think of the viscous sublayer as showing itself in mass transfer at high Schmidt numbers. This is mainly because if the Schmidt number is close to unity, Reynolds analogy applies, and the Stanton number would be approximately equal to the friction factor (over 2), whereas, at high Schmidt numbers the Stanton number times the Schmidt number to the 2/3 or 3/4 power is proportional to the square root of the friction factor. Nikuradse did a very good job of measuring the distribution of the eddy viscosity. There is no sign of a viscous sublayer. Nikuradse promoted the method of the universal law of resistance, plotting his friction-factor data in this way. Thus it was somewhat a surprise when integration of his eddy-viscosity data did not reproduce his friction-factor curve. It is quite a bit off.

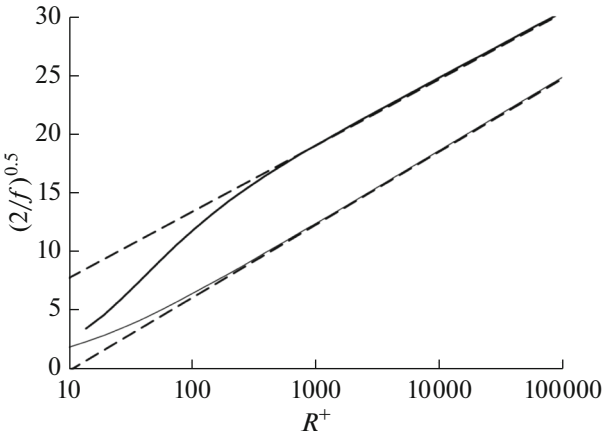

Fig. 5. Calculations of the friction factor from the distribution of eddy viscosity. The curve toward the bottom is obtained by direct integration of Eq. (3) with the eddy viscosity measured by Nikuradse, with smaller step sizes for larger values of R^+. The other curve was calculated with the dissipation program, in essence using the profiles of eddy viscosity in Fig. 3 but with inclusion of the y^3 region, the viscous sublayer. This curve rises from the lower curve and eventually approaches a straight line which is much higher than the asymptote with the lower curve. (Here Coef = 0.17, $n = p = q = 2$, $B^+ = 0.0005$. The curve is not modified when ε is nonzero and treated as in Fig. 3.) The straight lines are $(2/f)^{0.5} = 2.7 \ln(R^+) - 6.46$ for the lower line and $2.45 \ln(R^+) + 2$ for the upper line, which agrees well with Nikuradse's fit of experimental friction-factor data by means of the universal-resistance plot (see Eq. (B2)).

DISCREPANCIES

Nikuradse shows a nonzero eddy viscosity on the center line, unlike the dissipation theorem. This discrepancy has been resolved by modifying the decay term to reproduce Nikuradse's nonzero values of the

eddy viscosity on the axis. Nikuradse shows the friction factor following the asymptotic formula of the universal resistance law all the way down to $R^+ = 112$, while the dissipation theorem shows a negative deviation. See Fig. 5. At low values of R^+, Nikuradse's values of $\nu^{(t)}/\nu R^+$ tend to lie above the limit curve, but those for the dissipation theorem lie below. (Contrast Figs. 1 and 3.)

The decay term seems to call for an additive term of 4 to permit the equation of the dissipation theorem to be satisfied by the laminar flow (Poiseuille) result. It also arises by reverse engineering of Nikuradse's limit form for the eddy viscosity. However, it appears to be negligible at high levels of turbulence, and it can produce a profile of the eddy viscosity which is at variance with Nikuradse's measured profiles for the eddy viscosity (see Fig. 3).

The viscous sublayer is not yet integrated with the other regions, in the sense that we do not have a governing equation to determine the coefficient of the y^3 term, even though it is apparent that the viscous sublayer depends on and is closely related to the regions farther from the wall. Eddies in the outer flow are of significant size. These must decrease in size as the wall is approached. This is evident from the fact that the tangential average velocity approaches zero linearly as the wall is approached, and the normal average velocity approaches zero quadratically as required by the continuity equation. Near the wall, the nonlinear nature of the turbulence should be approached by governance of linear equations. Statistical theories of turbulence should help in developing a relationship between the B^+ parameter (characterizing the viscous sublayer) and ${B_1}^+$ (a calculated parameter characterizing the fluctuations farther from the surface and as predicted by the dissipation theorem). See, for example, [5]. We have not brought this to fruition here.

Despite these discrepancies, the agreement of the dissipation theorem with observed facts continues to get better.

CONCLUSIONS

The eddy viscosity appears not to go to zero on the axis of pipe flow, but instead has a small value. The friction factor can be calculated accurately by integration of the profile of eddy viscosity, but to get agreement with experiment, one needs to include the viscous sublayer very close to the solid pipe wall. One can derive the linear (asymptotic) relationship between the reciprocal of the square root of the friction factor and the logarithm of the stress parameter R^+ by careful examination of the form of the eddy viscosity near the solid wall. By reverse engineering, one can obtain a better idea of the behavior of the decay term in the dissipation theorem, thereby showing that the best value of n is 2 for the exponent on the volumetric dissipation. Hopefully, this work will lead to a better understanding of the decay term in other flow situations, including rotating cylinders and developing turbulent flows.

APPENDIX A

SINGULAR-PERTURBATION TREATMENT

Nikuradse's paper or Fig. 1 makes it clear that the eddy viscosity can be approximated by

$$M = \frac{\nu^{(t)}}{\nu R^+} = C\xi(1-\xi), \tag{A1}$$

where $C \approx 0.32$ and $\xi = r/R$. This formula appears to be uniformly valid in the wall, bulk, and core regions, that is, excluding the viscous sublayer. We shall use $C = 0.3$ when we need a numerical value. Formula (1) then provides interesting details of the profile of the volumetric dissipation.

Figure A1 shows that the core region and the bulk region can superpose if we use for the stretched radial variable $R^+\xi$ and for the stretched dissipation variable $(R^+)^2 D$. Figure A2 shows that the bulk region and the wall region can superpose if we use for the stretched radial variable $y^+ = R^+(1-\xi)$ and for the stretched dissipation variable D.

Equation (1) is general for pipe flow. In the bulk region, $\nu^{(t)} \gg \nu$ when R^+ is large, and the appropriate form for D is

$$D = \frac{\xi}{R^+ C(1-\xi)}. \tag{A2}$$

Thus, $D = O(1/R^+)$, and $\xi = O(1)$. As $\xi \to 0$, approaching the core, $D \to \xi/CR^+$, and, as $\xi \to 1$, approaching the wall region, $D \to 1/Cy^+$. These forms would be used when matching the bulk region with the core or the wall region. Note in connection with Fig. 3 that $DR^+ = O(1)$ in the bulk region.

The stretched coordinate in the core is $\overline{\xi} = R^+\xi$, and the appropriate form for D is

$$D = \frac{\overline{\xi}^2/(R^+)^2}{1 + C\overline{\xi}}. \tag{A3}$$

Thus, $D = O(1/(R^+)^2)$, and $\xi = O(1/R^+)$. As $\overline{\xi} \to \infty$, approaching the bulk, $D \to \overline{\xi}/C(R^+)^2$, demonstrating the matching between these two regions.

The stretched coordinate in the wall region is $y^+ = R^+(1-\xi)$, and the appropriate form for D is

$$D = \frac{1}{1 + Cy^+}. \tag{A4}$$

Thus, $D = O(1)$, and $1 - \xi = O(1/R^+)$. As $y^+ \to \infty$, approaching the bulk, $D \to 1/Cy^+$, demonstrating the matching between these two regions. Note that the thickness of the wall region is clearly shown here to be $\Delta\xi = O(1/R^+)$.

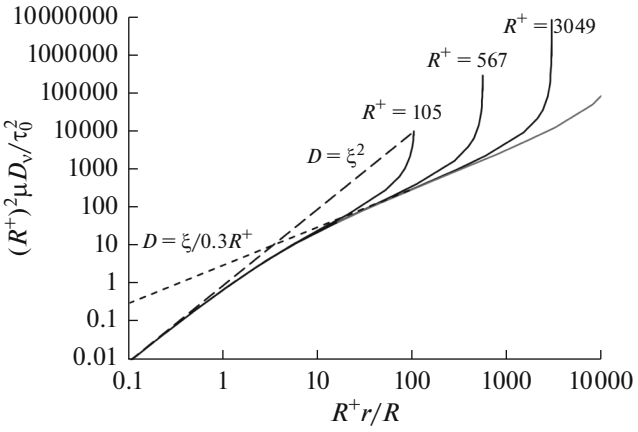

Fig. A1. Superposition of dissipation values in the core and bulk regions when using the proper stretched variables. $D = \xi/0.3R^+$ in the bulk region, and $D = \xi^2$ in the core region. The edge region shows deviation from this behavior.

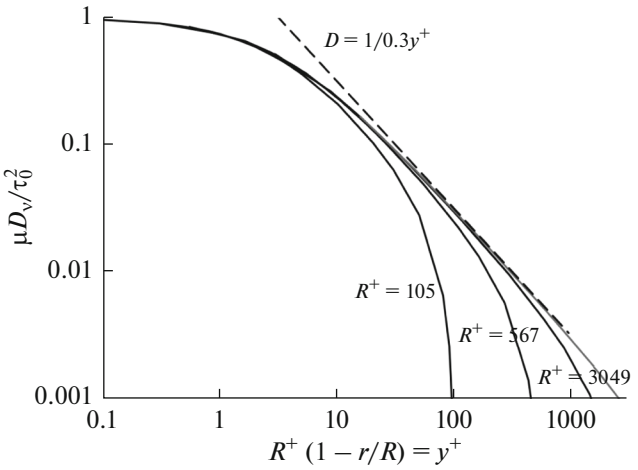

Fig. A2. Superposition of dissipation values in the bulk and wall regions when using the proper stretched variables. $D = 1/0.3y^+$ in the bulk region, and $D = 1/(1 + 0.3y^+)$ in the wall region. The core region shows deviation from this behavior.

It is expected that these orders of magnitude remain the same if we were using the dissipation theorem instead of assuming Eq. (A1) for the eddy viscosity. The conclusions should also remain the same if we used Eqs. (4) or (5) instead of Eq. (A1). The y^3 region (which in this case may be a y^4 region, see Appendix A of [2]) may be considered part of the law-of-the-wall region, and y^+ may still be the appropriate stretched variable. However, we are considering the y^3 region to be separate, since at present we have no way to treat it with the dissipation theorem. We do not have a valid governing equation in this region. The bulk is a region where $\nu^{(t)} \gg \nu$, whereas $\nu^{(t)} \approx \nu$ in the wall region. If $\nu^{(t)}$ went to zero on the center line, we could say that the core is a region where $\nu^{(t)} \approx \nu$. However, with Fig. 1 for the eddy viscosity not being zero on the axis, this is no longer true, and the core should be defined as the region where the volumetric dissipation is proportional to ξ^2.

Despite what is said in this appendix, Fig. 4 shows that the behavior of D is markedly different if we use Eq. (4) instead of Eq. (5). The curves for D still drop sharply, but then the slope decreases to 2 and the curve becomes parallel to the laminar line instead of bending over and approaching the laminar line asymptotically. Thus, a region with a slope of 1 does not exist in this case.

APPENDIX B

THE UNIVERSAL RESISTANCE FORMULA

For pipe flow, the universal resistance formula expresses the reciprocal of the square root of the friction factor as a linear function of the logarithm of the Reynolds number times the square root of the friction factor. This unlikely relationship may be thought of more simply as a linear relationship between the reciprocal of the square root of the friction factor and the logarithm of the stress parameter R^+. This can be carried over into the rotating-cylinder system and into mass transfer, at least at high Schmidt numbers (see [1] and [2]).

Nikuradse and also people before him recognized that the friction factor always has a lower slope at higher Reynolds numbers when plotted logarithmically but that a straight line results when data are plotted as mentioned above. Nikuradse extended the experimental Reynolds number to larger values and found a new asymptotic distribution for the eddy viscosity and for velocity profiles and the friction factor. He expressed his fit of the data for flow rate and pressure drop as

$$1/\sqrt{4f} = 2.0\log\left(\mathrm{Re}\sqrt{4f}\right) - 0.8, \qquad \text{(B1)}$$

which translates to

$$\sqrt{2/f} = 2.457\ln\left(R^+\right) + 1.9945. \qquad \text{(B2)}$$

The straight line for large values of R^+ can be derived as follows. From Eq. (17) of [2], the average velocity is

$$\left\langle \overline{\nu}_z \right\rangle = \frac{2}{R^2}\int_0^R \overline{\nu}_z r dr = \frac{\tau_0}{R^3}\int_0^R \frac{r^3 dr}{\mu + \mu^{(t)}}. \qquad \text{(B3)}$$

The definitions of Re, R^+, and f,

$$\mathrm{Re} = \frac{2R\left\langle \overline{\nu}_z \right\rangle}{\nu},\ R^+ = \frac{R}{\nu}\sqrt{\frac{\tau_0}{\rho}},\ \text{and}\ f = \frac{2\tau_0}{\rho\left\langle \overline{\nu}_z \right\rangle^2}, \qquad \text{(B4)}$$

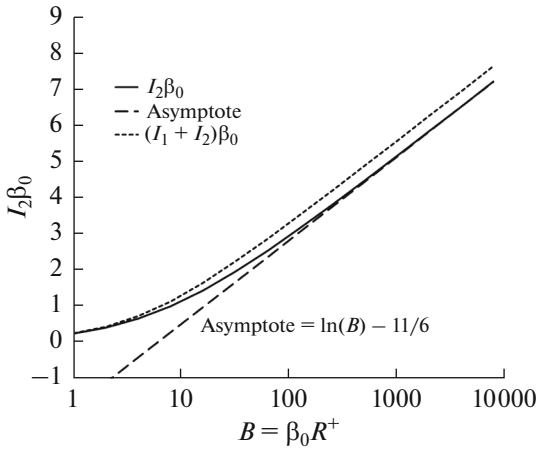

Fig. B1. The integral I_2 plotted both in its exact form and in the straight-line asymptote. The curve for $(I_1 + I_2)\,\beta_0$ is shown with short dashes.

produce a useful formula for calculating the friction factor from the eddy viscosity

$$\sqrt{\frac{2}{f}} = R^+\int_0^1 \frac{\xi^3 d\xi}{1 + R^+ M(\xi)}, \text{ where } \xi = r/R. \tag{B5}$$

A somewhat different formula applies to rotating cylinders. Even at large R^+ one cannot simply neglect the 1 in the denominator because M goes to zero at the pipe wall, $\xi = 1$. To account for the singularity let

$$M = (1 - \xi)\beta(\xi), \tag{B6}$$

where β_0 is the negative of the derivative of M at $\xi = 1$. Now, add and subtract the singular part of the integrand, so that Eq. (B5) becomes

$$\sqrt{\frac{2}{f}} = R^+\int_0^1 \left[\frac{\xi^3}{1 + R^+ M(\xi)} - \frac{\xi^3}{1 + \beta_0 R^+(1 - \xi)}\right] d\xi + R^+\int_0^1 \left[\frac{\xi^3 d\xi}{1 + \beta_0 R^+(1 - \xi)}\right]. \tag{B7}$$

Deal with the second integral first. Substitute $x = 1 + B(1 - \xi)$, where B stands for $\beta_0 R^+$ and is understood to be large.

$$I_2 = \frac{B}{\beta_0}\int_0^1 \frac{\xi^3 d\xi}{1 + B(1 - \xi)} = \frac{1}{B^3\beta_0}\int_1^{1+B} [B - x + 1]^3 \frac{dx}{x} = \frac{1}{B^3\beta_0}\int_1^{1+B} [(B + 1)^3 - 3x(B + 1)^2 + 3x^2(B + 1) - x^3]\frac{dx}{x}. \tag{B8}$$

Evaluation of the integral gives

$$I_2 = \frac{1}{B^3\beta_0}\left[(B + 1)^3 \ln(1 + B) - 3(B + 1)^2 B + 3(B + 1)\frac{(1 + B)^2 - 1}{2} - \frac{(1 + B)^3 - 1}{3}\right]. \tag{B9}$$

Further simplification leads to

$$I_2 = \frac{1}{B^3\beta_0}\left[(B + 1)^3 \ln(1 + B) - \frac{11}{6}B^3 - \frac{5}{2}B^2 - B\right]. \tag{B10}$$

We should retain this entire expression when we want the value of the friction factor without approximation. However, for the moment, just to get the straight-line expression, take B to be large and retain only a few terms.

$$I_2 = \frac{1}{\beta_0}\left[\ln(B) - \frac{11}{6}\right] = \frac{1}{\beta_0}\left[\ln(R^+) + \ln(\beta_0) - \frac{11}{6}\right]. \tag{B11}$$

Equations (B10) and (B11) are plotted in Fig. B1. The asymptote is good for $B > 512$. Since $\beta_0 \approx 0.4$, the approximation should be good for $R^+ > 2500$.

Equation (B11) establishes the slope of the straight line. For comparison with Eq. (B2), the slope is $1/\beta_0 = 2.708$ for my approximation to Nikuradse's original plot of eddy viscosity and 2.604 after I have modified the plot to go to zero at the center line. To get the additive constant, one also needs the first integral, which we evaluate numerically. The integrand is no longer singular.

$$I_1 = R^+\int_0^1 \left[\frac{\xi^3}{1 + R^+ M(\xi)} - \frac{\xi^3}{1 + \beta_0 R^+(1 - \xi)}\right] d\xi = R^+\int_0^1 \frac{\beta_0 R^+(1 - \xi) - R^+ M(\xi)}{[1 + R^+ M(\xi)][1 + \beta_0 R^+(1 - \xi)]}\xi^3 d\xi. \tag{B12}$$

This is the form to evaluate if you want no approximations. To get just the constant for the straight line valid for large R^+, make the approximation of taking R^+ to be large:

$$I_1 = \int_0^1 \frac{\beta_0 - \beta(\xi)}{\beta(\xi)\beta_0(1 - \xi)}\xi^3 d\xi = \int_0^1 \frac{\beta_0 - \beta(\xi)}{2\beta(\xi)\beta_0(1 - \xi)}\xi^2 d\xi^2. \tag{B13}$$

By expressing this as an integral over ξ^2, the integrand is nearly linear and is easy to integrate numerically. We use a spreadsheet to evaluate I_1, both approximately and by the exact equation. The approximation is independent of R^+ (as long as M is independent of R^+). The exact numerical integral is shown in Table B1, and the total integral is plotted dashed in Fig. B1.

With our evaluation, the universal resistance formula for pipe flow becomes

$$\sqrt{2/f} = 2.708\ln(R^+) - 6.46. \tag{B14}$$

Table B1. Values of integrals needed to calculate friction factors. $I_1\beta_0$ is about 3.26 at large values of R^+, but one cannot ignore the discussion of Fig. 5

B	$I_2\beta_0$	Asymp	$I_1\beta_0$
2	0.374	−1.140	0.235
4	0.623	−0.447	0.535
8	0.967	0.246	0.994
16	1.405	0.939	1.536
32	1.922	1.632	2.047
64	2.500	2.326	2.456
128	3.122	3.019	2.741
256	3.771	3.712	2.919
512	4.439	4.405	3.021
1024	5.117	5.098	3.076
2048	5.802	5.791	3.104
4096	6.490	6.484	3.119
8192	7.181	7.178	3.126
∞			3.257

The slope is close to Nikuradse's value, but the intercept is far off. In connection with Fig. 5, we discuss the numerical integration of Eq. (B5). We discovered, almost by accident, that the dependence of the eddy viscosity on radial distance in the viscous sublayer needs to be accounted for and that this leads to a substantially different value for the intercept. The slope may also be altered slightly. This reduces the usefulness of Table B1.

Figure B1 leads us to expect that the actual curve must deviate positively from the approximation, since it needs to approach zero at small values of R^+. Similarly, Fig. 11 of [2] should show negative deviations, whereas it shows a positive deviation. One possibility is that the value of B_1^+ becomes smaller for low values of R^+. This is observed with the dissipation theorem, but it is at variance with Nikuradse's observation that β_0 is independent of R^+. The matter is apparently resolved by the discussion of Fig. 5. The viscous sublayer needs to be taken into account, and the intercept to be used in the universal resistance law needs to be corrected toward the value given by Nikuradse in 1932.

This gives the asymptotic resistance relation. We have never seen it derived this way, although Prandtl, von Kármán, and Nikuradse and others were aware of the result and fitted parameters to the overall relationship between friction factor and Reynolds number from data on the flow rate for a given stress level over as large a range as possible.

We notice from this exercise, that it is the values of eddy viscosity near that wall that are most important in determining the fraction factor. We see this first in the universal resistance law, where the coefficient of the logarithmic term is largely determined by the slope of the eddy-viscosity curve near the wall (see β_0). We see this again when we see that the intercept of the universal resistance law is largely determined by the eddy viscosity in the y^3 region.

REFERENCES

1. Newman, J., Theoretical analysis of turbulent mass transfer with rotating cylinders, *J. Electrochem. Soc.,* 2016, vol. 163, p. E191.
2. Newman, J., Application of the dissipation theorem to turbulent flow and mass transfer in a pipe, *Russ. J. Electrochem.*, 2017, vol. 53, p. 1061.
3. Nikuradse, J. Gesetzmässigkeitem der turbulentem Strömung in glaten Rohren, Forschungsheft 356, Beilage zu Forschung auf dem Gebiete des Ingenieurwesens, Edition B, Volume 3, September/October, 1932 (Berlin NW7:VDI-Verlag GMBH, 1932). Translated as Nikuradse J., Laws of turbulent flow in smooth pipes, *NASA TT F-10, 359,* Washington: National Aeronautics and Space Administration, Oct. 1966.
4. Cahn, J. W. and Hilliard, J. E., Free Energy of a nonuniform system. I. Interfacial free energy, *J. Chem. Phys.*, 1958, vol. 28, pp. 258–267. doi 10.1063/1.1744102
5. Martemianov, S.A., Statistical theory of turbulent mass transfer in electrochemical systems, *Russ. J. Electrochem.*, 2017, vol. 53, p. 1076.